Chapter 27
Vascular Flow Modelling Using Computational Fluid Dynamics

Amir Keshmiri and Kirstie Andrews

27.1 Computational Fluid Dynamics

The equations governing fluid flows are a set of coupled, non-linear partial differential equations such as:

27.1.1 Continuity

$$\frac{\partial \rho}{\partial t} + \frac{\partial \rho U_i}{\partial x_i} = 0 \tag{27.1}$$

27.1.2 Momentum

$$\frac{\partial \rho U_i}{\partial t} + \frac{\partial \rho U_i U_j}{\partial x_j} = \frac{\partial P}{\partial x_j} + \frac{\partial}{\partial x_j}\left(\mu \frac{\partial U_i}{\partial x_j}\right) \tag{27.2}$$

A. Keshmiri (✉)
School of Engineering, Manchester Metropolitan University, Manchester M1 5GD, UK

School of Mechanical, Aerospace and Civil Engineering, The University of Manchester, Manchester M13 9PL, UK
e-mail: a.keshmiri@mmu.ac.uk

K. Andrews
Division of Mechanical Engineering, School of Engineering, Manchester Metropolitan University, Manchester M1 5GD, UK
e-mail: k.andrews@mmu.ac.uk

M. Slevin, G. McDowell (eds.), *Handbook of Vascular Biology Techniques*,
DOI 10.1007/978-94-017-9716-0_27

These equations are known as Navier–Stokes equations. Many real problems include additional terms and/or equations, governing heat transfer, chemical species, etc. Analytical solutions are known only for a few very simple flow cases. An alternative is to solve the governing equations numerically, on a computer. Computational Fluid Dynamics (CFD) is this process of obtaining numerical approximations to the solution of the governing fluid flow equations.

One could view CFD as *a numerical experiment*. In a typical fluids experiment, an experimental model has to be built and the flow interacting with that model needs to be measured using various measurement devices, and the results are then analysed. In CFD, the building of the model is replaced with the formulation of the governing equations and the development of the numerical algorithm. The process of obtaining measurements is replaced with running an algorithm on the computer to simulate the flow interaction. The analysis of the results is, however, the same for both techniques. There are several unique advantages of CFD over experiment-based approaches:

- **Relatively low cost:** Using physical experiments and tests to get essential engineering data for design can be expensive. CFD simulations are relatively inexpensive, and costs are likely to decrease as computers become more powerful.
- **Speed:** CFD simulations can be executed in a short period of time. Quick turnaround means engineering data can be introduced early in the design process.
- **Ability to simulate real conditions:** Many flow and heat transfer processes cannot be (easily) tested, e.g. hypersonic flow. CFD provides the ability to theoretically simulate any physical condition.
- **Ability to simulate ideal conditions:** CFD allows great control over the physical process, and provides the ability to isolate specific phenomena for study. For example extreme pressures or temperatures can easily be simulated.
- **Comprehensive information:** Experiments only permit data to be extracted at a limited number of locations in the system (e.g. pressure and temperature probes, heat flux gauges, etc.). CFD allows the analyst to examine a large number of locations in the region of interest, and yields a comprehensive set of flow parameters for examination.

However, despite its many advantages, CFD does not remove the need for experiments; numerical models need to be validated to ensure they produce reliable and accurate results. Particularly in clinical applications, there is a pressing need for rigorous model validation against detailed laboratory data. With the growth of available computing power and the advent of powerful user-friendly graphical user interfaces and automated options/features in commercial CFD codes, it has become possible for a wide range of users to apply CFD to even very complex flowfields, giving detailed information about the velocity field, pressure, temperature, etc. This sometimes results in producing solutions that are haemodynamically irrelevant and fail to capture even the most basic flow features. The key to successful use of CFD is an understanding of where the errors come from; their implications, and how to ensure they are small enough to be acceptable in a particular application.

27.2 Applications of CFD

27.2.1 Disease Research

In recent years, advances in vascular biology, biomechanics, medical imaging and computational techniques including CFD have provided the research community with a unique opportunity to analyse the progression of vascular diseases from a new angle and to improve the design of medical devices and develop new strategies for intervention. The increasing power-to-cost ratio of computers and the advent of methods for subject-specific modelling of cardiovascular mechanics have made the CFD-based modelling sometimes even more reliable than methods based solely on in vivo measurement.

Numerical simulations have played an important role in understanding the haemodynamics of several different areas including bypass grafting, cardiovascular treatment planning, cerebrovascular flow, the effects of exercise on aortic flow conditions, congenital heart disease and coronary stents. The patient-specific modelling of cardiovascular mechanics, however, have focused mainly on haemodynamic factors in atherosclerotic and aneurysmal disease.

Atherosclerosis, is the most widespread of the acquired cardiovascular diseases and affects various arteries supplying blood to brain, heart and other vital organs. It is a very focal disease, mainly affecting branches and bends of the arterial tree. There is currently extensive and increasing evidence, correlating the localisation of atherosclerosis and the patchiness of this disease to different local haemodynamic metrics [1] (see Sect. 27.4, below). Currently the majority of the research with an aim of correlating the haemodynamic parameters to the formation of atherosclerosis are based on the coronary arteries and the carotid bifurcation models of human, porcine, rabbit and murine [2]. Quantification of haemodynamic metrics in rodent models have recently become more feasible with the advent of small-animal imaging technology, advanced image-based modelling techniques and genetic manipulation. These models are particularly useful for studying atherosclerosis since the wall shear stress in the aorta of a mouse is more than 20-fold higher than that in humans [3].

In addition to atherosclerosis, aneurysm is another important disease which has been studied extensively in the literature. An aneurysm is defined as a focal dilatation of the arterial wall. Although the pathogenesis of aneurysms remains an enigma, the initial dilatation appears to be caused in part by degeneration of a portion of the arterial wall. There are two main types of aneurysms, namely Intracranial Aneurysms (IAs) and Abdominal Aortic Aneurysms (AAAs). IAs mostly occur at the circle of Willis, the major network of arteries that supplies blood to the brain. The major complication of IAs is their rupture, which causes subarachnoid haemorrhage. AAAs occur in the infrarenal aorta, the primary conduit that supplies blood to the legs. Similar to studying atherosclerosis, image-based computational modelling using CFD has recently been used extensively to calculate the haemodynamic forces and to correlate them to initiation, growth and rupture of aneurysms. Recent studies

using CFD have shown the importance of haemodynamic metrics in understanding cerebral aneurysm rupture [4, 5]. Amongst several haemodynamic parameters calculated by CFD, Miura et al. [6] found the wall shear stress to be the most reliable parameter characterising the rupture status of middle cerebral artery. The review by Humphrey and Taylor [7] provides a thorough review of the role of computational mechanics in both types of aneurysms.

27.2.2 Predictive Medicine

In treating cardiovascular problems, interventional and surgical therapies are critical for restoring blood flow to affected organs and tissues. However, adverse and side effects from these therapies have always been a limitation. In addition, using a "trial-and-error" approach to surgical design is obviously not an option which limits testing alternate treatments in the patients. The recent developments in patient-specific computer simulations have provided a means to assess new surgeries and interventions at no risk to the patient. Also similar to other engineering fields such as aerospace and automotive, design optimisation is now possible and can be applied to predictive tools and methods to optimise surgeries for individual patients. Therefore, in the new paradigm of predictive medicine, the surgeons for example may use advanced imaging tools along with computational techniques such as CFD to create a patient-specific model and predict the outcome of a particular treatment for an individual patient. However, to be effective and attractive to the medical community, these simulation-based medical planning systems must be quick and efficient and should require minimum user intervention. They should also accurately calculate relevant haemodynamic variables, especially flow rate and pressure [8]. Such systems would require a number of key stages, which are briefly discussed in Sect. 27.3.

Another new and active area of research in which CFD and computational haemodynamic can play an important role is the design and clinical use of *artificial blood vessels*. While it is considered as a long-standing therapy, with the growth of multi-disciplinary fields such as biomaterials and tissue engineering, researchers are looking to provide clinicians and patients with enhanced options when repairing or replacing these structures. The artificial tissue analogues may be polymeric tubes (similar to the current "gold standards" of Dacron (i.e. polyethylene terephthalate, PET) or expanded polytetrafluoroethylene – ePTFE) or tissue engineered vessels ((degradable) polymeric tubes seeded with layers of vascular cells designed to regenerate into a fully formed structure that will mimic the natural healthy vessel) [9, 10]; whichever is chosen, the likely success of the replacement vessel needs to be analysed.

CFD has recently shown potential to provide researchers with valuable information regarding the forces, stresses and haemodynamic factors that will affect the

specific anatomical location of the artificial vessel, for example the wall shear stress. It is critical to have this information as these variables will not only affect the material of the vessel wall, but also the contacting cells. As discussed in Chap. 25, the endothelialisation of artificial vessels is a key component of finding a bioengineered solution to the vascular problem of damaged and diseased blood vessels. As these cells form a critical layer between the circulating blood and the artificial underlying material layer(s), the haemodynamic factors they are exposed to, will directly induce cell responses ranging from preferential adaptation and alignment to inflammatory responses and detachment. The endothelial cells attachment and responses can be controlled to an extent through the alteration of the underlying artificial material structures; therefore, if the full environment of the artificial vessel, in its specific location, is understood beforehand then the forces, stresses and haemodynamic factors present can be factored into the design. The vessel substitutes not only need to withstand the applied forces/stresses but also need to produce and replicate the behaviour of natural healthy vessels as closely as possible to prevent anastomosis mismatch, subsequent cell loss, and poor haemodynamic performance [11, 12]. Hence, CFD provides a tool with vast potential for improving clinical therapeutic solutions, and is an area that, if more widely incorporated, can significantly contribute to the knowledge and development of artificial blood vessels. (Further details regarding the potential to directly affect the endothelialisation through the underlying material structural properties are discussed in Chap. 25.)

27.3 Computational Procedure

A typical CFD simulation consists of the following tasks:

1. Problem Identification
2. Pre-processing
3. Solving
4. Post-processing

These tasks are discussed below in more detail.

27.3.1 Task 1: Problem Identification

The first step in any CFD simulation is to define the modelling goals and subsequently identify the numerical domain that needs to be modelled.

In defining the modelling goal, the following points need to be considered**:**

- Decide if CFD is an appropriate tool
- Choose the modelling options

  - The physical models needed for analysis (i.e. turbulence, heat transfer, compressibility, etc.)
  - The simplification assumptions (i.e. steady-state, symmetry, periodicity, etc.)
  - Unique modelling capability (i.e. Graphical User Interface, special features of a code, etc.)
- Choose the degree of accuracy
- Choose how quickly the results are needed

When identifying the flow domain, the following need to be taken into consideration:

- Decide how to choose the computational domain
  - Known boundary conditions and other input data
  - Extension of domain to enable comparison with data
- Decide if you can simplify the domain (e.g. 1D, 2D, etc.)

27.3.2 Task 2: Pre-processing

The pre-processing stage is normally the most time-consuming task in a CFD simulation, especially in vascular flow problems. The purpose of this task is essentially to prepare the flow problem before the governing equations of the flow can be solved computationally. The pre-processing typically consists of the following two main stages:

1. Definition of the geometry of the region of interest: *Computational Domain (or Geometry)*
2. Sub-division of the domain into a number of smaller, non-overlapping sub-domains: *Mesh (or Grid)*

Each stage is explained in more detail below.

27.3.2.1 Computational Domain

The computational domain which is usually based on a CAD (Computer-Aided Design) file, is a computer model to represent the fluid domain. In cardiovascular problems, there are different invasive and non-invasive techniques to acquire patient-specific anatomic and physiologic data. Common invasive methods include a combination of angiography and intravascular ultrasound (IVUS). Non-invasive imaging is usually carried out by Computerised Tomography (CT), Magnetic Resonance Imaging (MRI) and 3-Dimensional Ultrasound (3DUS). One of the advantages of MRI over other techniques is its ability to measure physiologic parameters such as blood flow and wall motion [8]. However, there are two major limitations in the computational imaging techniques which are namely

Table 27.1 List of current biomedical modelling codes (Adapted from [17])

Software	Ref.	Capabilities		
		Segmentation	Rendering	Simulation
ImageJ	[14]	✓	✓	×
SimVascular	[15]	✓	✓	✓
VMTK	[16]	✓	✓	✓

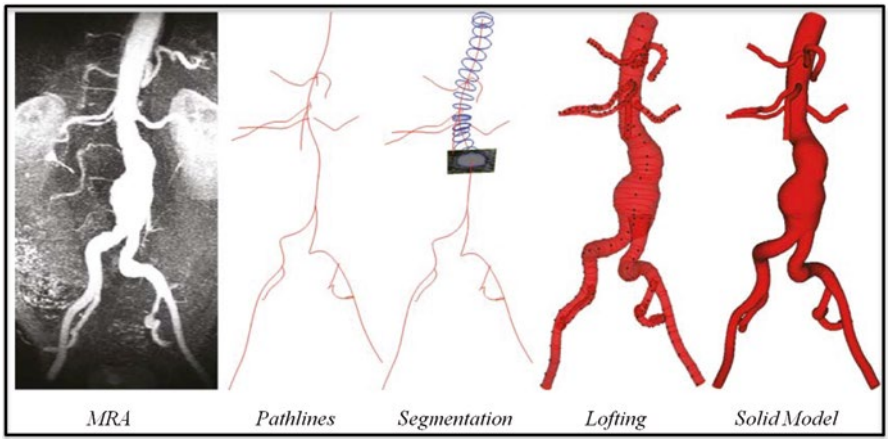

Fig. 27.1 Steps involved in creating a solid model from magnetic resonance angiography (MRA) for an abdominal aortic aneurysms (Adapted from [18])

the relatively low resolution of current imaging tools and geometrical variations during a cardiac cycle [13].

Following the acquisition of patient specific anatomic data, the computational domain can be created using a number of different software/codes. Table 27.1 lists three of the most common codes currently being used for creating a CAD model from medical images.

The solid model of, for example a blood vessel in these codes is typically created through the following steps [8]:

1. Obtaining a volume-rendered image of the area of interest usually by a contrast-enhanced magnetic resonance angiogram (MRA).
2. Creating centre-line paths along the vessels of interest.
3. Taking two-dimensional segmentations of vessel lumen perpendicular to the vessel path.
4. Lofting (or sweeping) the two-dimensional segmentations to form solid models for each vessel
5. Joining the different solid models of each vessel to form a complete three-dimensional solid model (which is ready to be meshed).

Figure 27.1 shows the application of the above steps for creating a typical abdominal aortic aneurysm (AAA) solid model.

27.3.2.2 Meshing

Once the computer model (or the CAD file) based on imaging data was created, the next step is to generate a mesh (or a grid). The mesh generation process consists of sub-dividing the domain into a number of smaller, non-overlapping sub-domains (known as 'cells', 'control volumes' or 'elements'). Meshing is needed since the numerical solution of the fluid flow governing equations cannot produce a continuous distribution of the variables (e.g. velocity, pressure, temperature etc.) over the whole computational domain, thus the aim instead becomes to produce a set of discrete values at a number of cells that cover the solution domain. In other words, the mesh designates the cells or elements on which the flow is solved and is a discrete representation of the geometry of the problem.

There are broadly two types of mesh: (1) structured and (2) unstructured. As shown in Fig. 27.2, structured grids are ideal for simple geometries and for simulations carried out using in-house CFD codes and therefore are rarely used in cardiovascular flow problems. Unstructured meshes (shown in Fig. 27.3) on the other hand, can accommodate completely arbitrary geometries; however, there are penalties to be paid for this flexibility, both in terms of the connectivity data structures and solution algorithms.

The mesh has a significant impact on the rate of convergence (i.e. reaching a solution), solution accuracy and the required computational time. In general, the

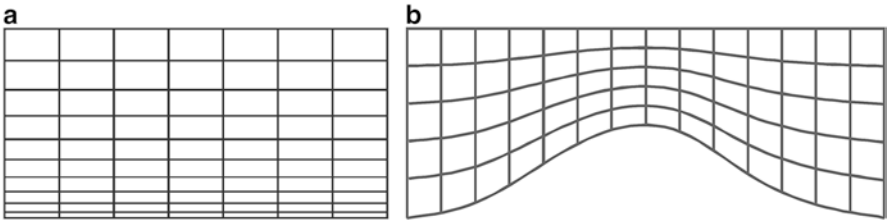

Fig. 27.2 Schematic of a typical structured mesh; (**a**) Cartesian and (**b**) Curvilinear

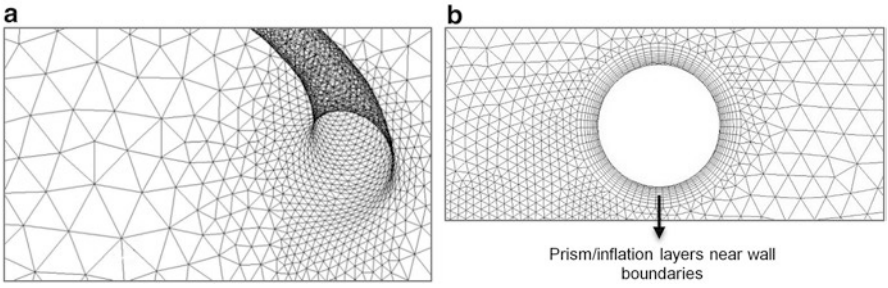

Fig. 27.3 Examples of typical unstructured grids; (**a**) tetrahedral mesh for an aorta with an intercostal branch, and (**b**) tetrahedral mesh with prism/inflation layers around a circular wall boundary

Table 27.2 List of popular mesh generation codes available in the market

Product(s) name	Developer	Mesh type
Gambit	Ansys	Finite volume
Ansys-meshing	Ansys	Finite volume
ICEM-CFD	Ansys	Finite volume
T-grid	Ansys	Finite element
STAR-CD+	CD-Adapco	Finite volume
HyperMesh	Altair	Finite element
PATRAN	MSC software	Finite element

larger the number of cells/elements, the better the solution accuracy. The number of cells in the mesh would have direct effects on the computational time and cost and therefore, the mesh resolution needs to be optimised to improve efficiency. As a general rule, the mesh needs to be finer in areas where large variations occur (e.g. near-wall regions) and coarser in regions with relatively little change. The mesh adjacent to the wall boundaries is particularly important as it needs to be fine enough to resolve the boundary layer flow. In addition, in unstructured grids, in near-wall regions, rectangular/quadrilateral cells (so called prism/inflation layers) are preferred over other shapes (see Fig. 27.3b).

It is difficult to create a comprehensive list of rules for generating an optimum mesh and hence, it is the skills and the experience of the user which play an important role. Nowadays, the majority of commercial mesh generation packages are equipped with semi-automatic mesh generation tools which enable even novice users to create acceptable grids within hours. Table 27.2 provides a list of common mesh generation programmes which are commonly used for biomedical and bioengineering CFD simulations and can create grids which are based on Finite Volume or Finite Element (explained in more detail in Sect. 27.3.3.2, below).

27.3.3 Task 3: Physical Definition and Solving

As the most crucial step in a CFD process, Task 3 is where the user is required to have expertise in a number of areas including fluid mechanics (e.g. mass and momentum conservation, incompressible flow, non-Newtonian flows, turbulence etc.), numerical methods (e.g. discretization, solution methods etc.), heat transfer (e.g. conduction, diffusion, advection etc.) and programming (e.g. C++, Fortran, Python etc.). The latter is nowadays probably not as important anymore thanks to the significant improvements made to the Graphical User Interfaces (GUI) in most CFD codes with an aim of making these tools available to a wider range of users.

Table 27.3 provides a list of popular CFD codes which are also commonly used for biomedical simulations.

One could generally divide Task 3 into the following two stages:

1. Defining the physical and boundary conditions: *Numerical Input*
2. Computing and monitoring the solution: *Solving*

Table 27.3 List of popular CFD codes currently available for biomedical CFD simulations

Product(s) name	Developer	Type
Fluent, CFX	Ansys	Commercial
STAR-CD, STAR-CCM+	CD-Adapco	Commercial
OpenFOAM	OpenCFD	Open-source
FLOW3D	Flow Science	Commercial
PHOENICS	CHAM	Commercial

Both of these stages (described further below) are carried out within the same code/package. The majority of the current commercial CFD codes make use of CAD-style graphical user interface to enable the user to import data from proprietary surface modellers and mesh generators and enter the numerical input. In addition to Navier–Stokes and energy equations, the CFD codes generally allow the user to also solve extra equations and models for special physical and chemical processes.

27.3.3.1 Numerical Input

Once the mesh is created or imported into the CFD code, the next step is to set up the physics of the flow through defining physical models, material properties, domain properties, solver settings and boundary conditions. In vascular flow modelling for instance, the latter usually encompasses most of the input information related to the patient including heart rate, blood pressure, blood flow velocity and temperature which may be obtained through invasive or/and non-invasive measurement techniques. The boundary conditions for a typical cardiovascular flow problem tend to incorporate upstream heart models and downstream microcirculation models too. The main types of boundary conditions in a typical CFD simulation include inlet, outlet, wall, symmetry[1] and cyclic (periodic).[2] Figure 27.4 shows an example of employing cyclic and symmetry boundary conditions in the simulation of a ribbed channel flow which results in the reduction of the computational domain i.e. less computational time and power required. The properties of the blood flow such as density, viscosity and temperature, etc. would also need to be defined as part of the material properties. Other numerical inputs include solver settings (e.g. numerical schemes, convergence controls, etc.), the discussion of which is beyond the scope of this chapter and the interested reader is referred to Peric and Ferziger [19] for further information.

[1] Symmetry boundary conditions are those that arise by viewing the computational domain as a sub-region of some larger domain which possesses planes or axes of symmetry.

[2] This type of boundary condition consists of pairs of geometrically identical boundaries at which all flow conditions are matched.

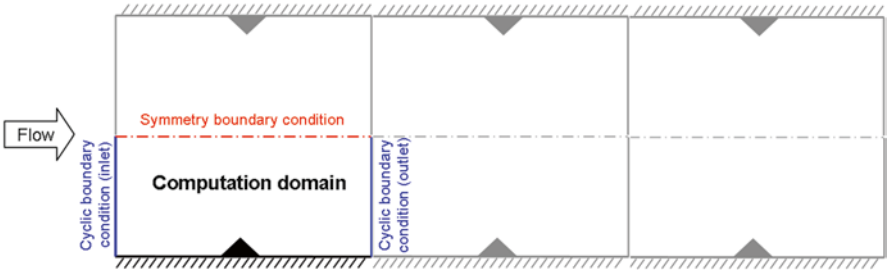

Fig. 27.4 An example of using cyclic and symmetry boundary conditions to reduce the computational domain

27.3.3.2 Solving

This is the step where the equations that govern the blood flow are solved. In summary, solving the main governing equations involves the following phases [20]:

1. *Approximation* of the unknown flow variables by means of simple functions.
2. *Discretisation* by substitution of the approximations into the governing flow equations and subsequent mathematical manipulations.
3. *Solution* of the algebraic equations.

A vast majority of the current CFD codes are based on one of the following three main numerical solution techniques: (1) Finite Difference, (2) Finite Element and (3) Finite Volume. The main differences between these techniques are associated with the way in which the flow variables are approximated and then discretised.

Finite difference is commonly used in in-house codes and simple structured CFD problems due to its simplicity and its application, therefore, is restricted to simple classical test cases (e.g. channel flows, pipes, etc.). While the finite element method is mainly used for structural stress analysis, it has some distinctive features such as its abilities to deal with arbitrary geometries which makes it somewhat attractive in vascular flow simulation problems. Finite element is not well-suited for turbulent flows and since the majority of haemodynamic problems involve laminar flow, it is often used in in-house codes which are developed mainly for biofluid/biomedical problems. However, it is the finite volume method (which was originally developed as a special finite difference formulation) that is currently the most popular technique in CFD. More detailed information about these three techniques can be found in several text books including Peric and Ferziger [19].

27.3.4 Task 4: Post-processing

The purpose of the post-processing task is to visualise the simulation results and to quantify the resulting physiological information. There are several different techniques and tools to enable the CFD user to extract desirable results. The majority of

the commerical CFD packages allow the user to export the results in different formats which can then be analysed using more specialist programmes such as Ansys-Post, MATLAB, Tecplot, EnSight, ParaView, AVS, etc. or even simpler programmes such as Microsoft Excel or Xmgrace for simple 2D plots. However, nowadays the majority of the commercial CFD codes have post-processing capabilities within their GUI which are ideal for quick examination of the results and producing basic images and even animations. The most common types of visualisation tools include line and shaded contour plots, vector plots, streamlines/pathlines, 2D plots, etc. In biomedical applications, contour plots are probably the most common tool to show the simulations results at different locations within the computational domain (see Fig. 27.7, for example).

Figure 27.5 shows an overview of the steps involved in a typical vascular CFD flow problem.

27.4 Haemodynamic Parameters

As was alluded to in Sect. 27.2.1 above, in the computational haemodynamics there are several different haemodynamic parameters/metrics which are mainly used to identify the distribution of atherosclerotic lesions within the arterial system or the rupture of aneurysms. These haemodynamic parameters can be directly derived from the flow fields obtained by CFD-based simulation tools. The reason for having to define different metrics for the variation in blood flow characteristics is mainly due anatomic and physiologic variations and system complexity of the fluid flow as well as its interaction with the vessel wall and tissue. In addition, single-feature-haemodynamic metrics are generally unable to capture the multi-directionality of the flow field [22], hence, having to define different parameters.

This section discusses the most common haemodynamic parameters currently used in the literature.

27.4.1 Wall Shear Stress (WSS)

The Wall Shear Stress (WSS) or τ_w is the most common haemodynamic parameter and refers to the tangential, frictional stress exerted by the action of blood flow on the vessel wall. In fluid mechanics shear stress (expressed in Pascal, *Pa*) is the resultant force (per unit area) which arises from the friction between two layers of the fluid moving at different velocities. In vascular flows, there is normally significant shear stress between blood flow and the endothelial layer which results in shearing deformation of the endothelial cells.

For a typical laminar blood flow with parabolic velocity profile, the shear stress may be written as

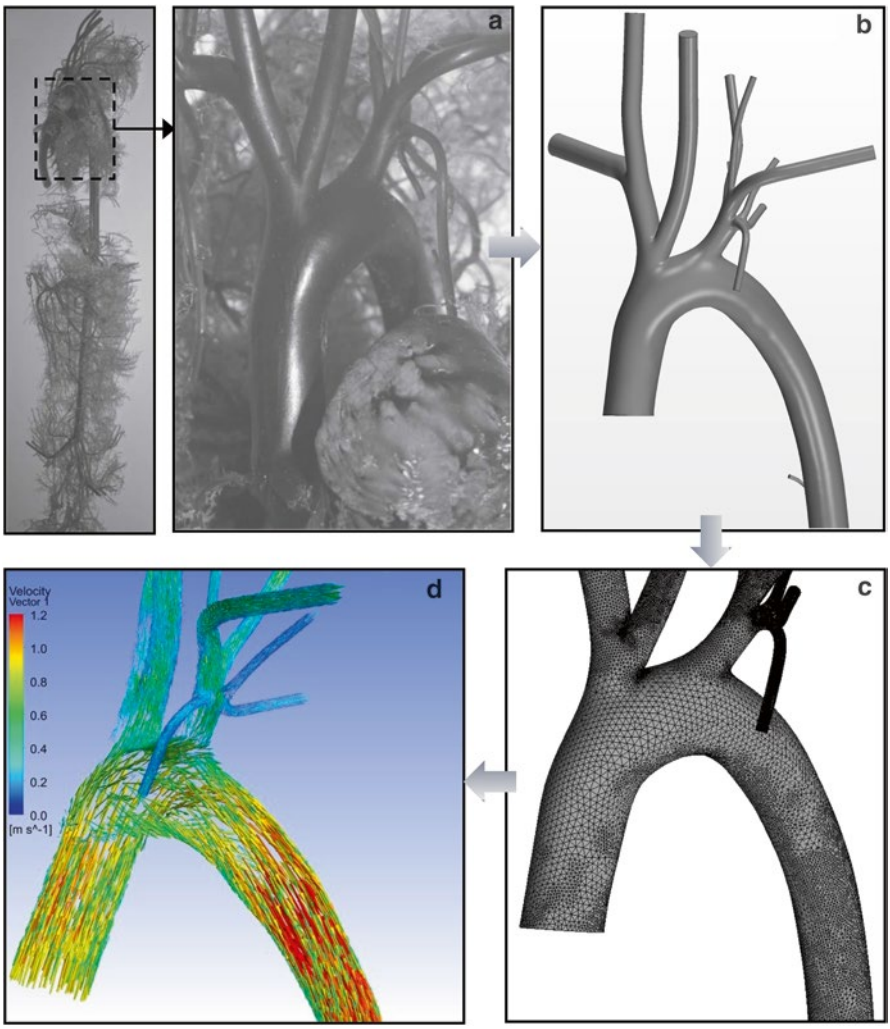

Fig. 27.5 A typical example of a CFD process for a rabbit aortic arch and descending thoracic aorta: (**a**) A ventral–dorsal view of the entire resin cast prepared for the CT scanner (taken from [21]), (**b**) the solid computer model (created using VMTK), (**c**) an unstructured tetrahedral mesh (prepared by ICEM-CFD) and (**d**) post-processing of the simulation results using a velocity vector plot (simulations carried out by Ansys-Fluent and the results post-processed by Ansys-Post)

$$\tau = \frac{4\mu Q}{\pi r^3} \tag{27.3}$$

where Q is the flow rate, normally expressed in dyn/cm^2 (where 1 dyn = 10^{-5} N). Vascular shear stress of large conduit arteries typically varies between 5 and 20 dyn/cm^2. In large and straight blood vessels, this continuous exposure to a physiologic range

of shear stress promotes the establishment of important physiologic characteristics of the artery wall promoting an anti-inflammatory, anti-thrombotic, anti-coagulative, profibrinolytic and anti-hypertrophic state [23].

As shown in Fig. 27.6a, for laminar flow of a Newtonian[3] fluid, the shear stress is simply proportional to the velocity gradient ($\partial u/\partial r$) and the fluid viscosity (μ):

$$\tau = -\mu \frac{\partial u}{\partial r} \tag{27.4}$$

and consequently the wall shear stress is the value of the shear stress evaluated at the wall:

$$\mathrm{WSS} = \tau_w = \tau(R) = -\mu \left(\frac{\partial u}{\partial r} \right)_{wall} \tag{27.5}$$

In cardiovascular problems, due to the transient (pulsatile) nature of the blood flow, it is more useful to define the time-averaged WSS (TAWSS) which is calculated by integrating the WSS magnitude at each geometric part over the cardiac cycle:

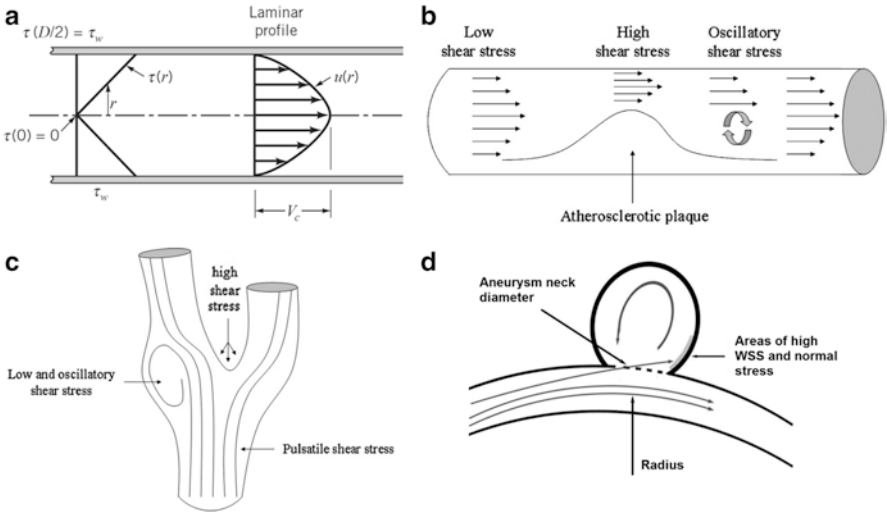

Fig. 27.6 (**a**) schematic of velocity profile and shear stress distribution within the blood flow in a typical artery [26], (**b**) distribution of shear stress in a straight arterial segment proximal to a lumen-protruding atherosclerotic plaque [27], (**c**) distribution of wall shear stress in a typical carotid artery bifurcation [28], and (**d**) schematic representation of an aneurysm originating on the outer curve of an intracranial artery; areas adjacent to the impact site experience high levels of wall shear stress [29]

[3] Fluids for which the shearing stress is *linearly* related to the rate of shearing strain (also referred to as rate of angular deformation) are designated as *Newtonian fluids.* On the other hand, fluids for which the shearing stress is not linearly related to the rate of shearing strain are designated as *non-Newtonian fluids.* Blood is a non-Newtonian fluid, even though for simplicity it is usually assumed to be a Newtonian fluid in most CFD simulations.

$$\mathrm{TAWSS} = \frac{1}{\mathrm{T}} \int_0^T |\vec{\tau}_{\mathrm{w}}| \, \mathrm{dt} \tag{27.6}$$

where $\vec{\tau}_{\mathrm{w}}$ is the instantaneous wall shear stress vector, t is the time and T is the duration of the cardiac cycle.

The relationships between the wall shear stress and distribution of atherosclerotic lesions in the arterial system has been the subject of several research papers in the past five decades with some contradicting conclusions. For instance, by studying hypercholesterolaemic animals, Fry [24] suggested that high WSS leads to endothelial damage and hence increases lipoprotein influx into the intima. On the other hand, through studying human post-mortem material, Caro et al. [25] proposed that high WSS was rather protective and found that atherosclerotic lesions instead occur in regions of low WSS. Recently, Peiffer et al. [2] carried out a systematic review of several papers and found that the majority of the studies support the low WSS theory. However, the presence of a direct correlation between lesions and WSS is probably too simplistic, hence suggesting a need for more complex haemodynamic metrics based on deeper understanding of arterial flow physics and its interaction with the endothelial cells and layers.

The significance of shear stress-based metrics in different vascular problems are depicted in Fig. 27.6b–d which show the expected shear stress distributions in a lumen protruding artery, a carotid artery bifurcation and an aneurysm, respectively.

An example of TAWSS magnitude calculated by CFD for rupture-predictions in intracranial aneurysms shown in Fig. 27.7. In Sect. 27.4.3, two more examples of TAWSS are given (Fig. 27.8) for the atherosclerosis localisation in the descending thoracic aorta.

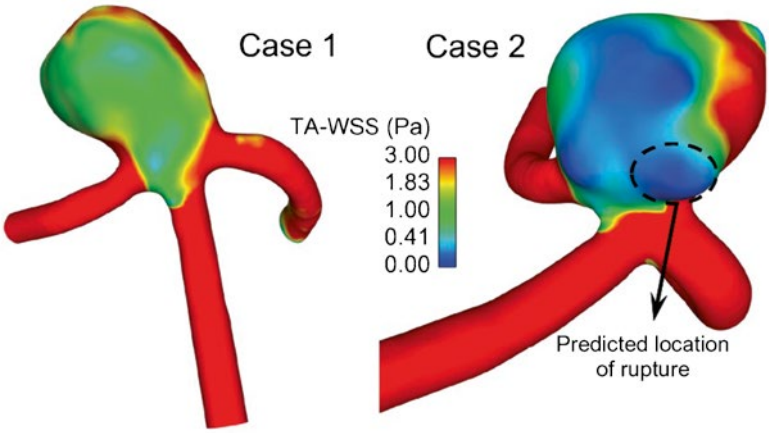

Fig. 27.7 Rupture prediction in two patient-specific intracranial aneurysms using predicted time-averaged wall shear stress magnitude. CFD simulations of both cases suggest that Case 2 is more likely to rupture based on low shear theory (the aneurysm models were provided by [30])

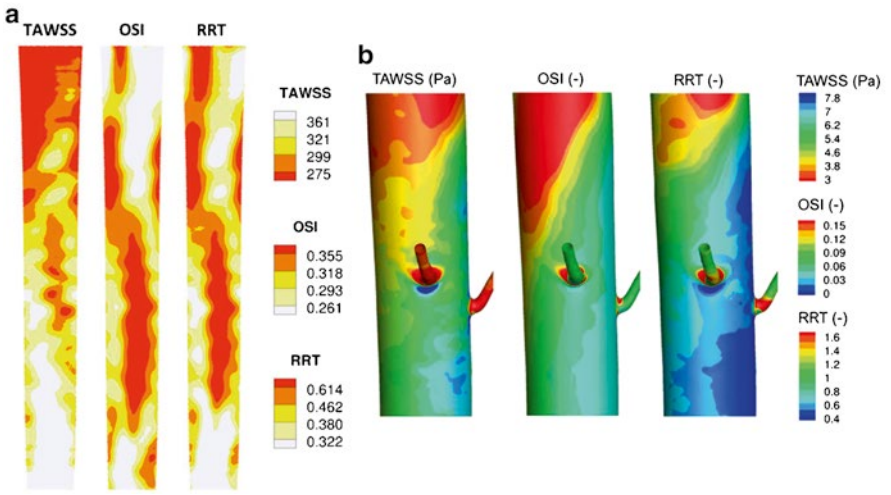

Fig. 27.8 Distribution of three haemodynamic metrics; (**a**) descending thoracic aorta of a mouse with aortic valve regurgitation (Modified from [34]); (**b**) close-up of the proximal left intercostal branch ostium in a rabbit aorta (Modified from [22])

27.4.2 Oscillatory Shear Index (OSI)

In addition to wall shear stress, in 1980s, Ku et al. [31] identified another haemodynamic metric known as Oscillatory Shear Index (OSI) which was associated with the flow reversal. A more common definition of OSI, generalised for three dimensional flows, was proposed by He and Ku [32] as

$$\mathrm{OSI} = \frac{1}{2}\left(1 - \frac{\left|\int_0^T \vec{\tau}_w \mathrm{d}t\right|}{\int_0^T |\vec{\tau}_w| \,\mathrm{d}t}\right) = \frac{1}{2}\left(1 - \frac{\left|\vec{\tau}_{mean}\right|}{\mathrm{TAWSS}}\right) \tag{27.7}$$

where

$$\vec{\tau}_{mean} = \frac{1}{\mathrm{T}}\int_0^T \vec{\tau}_w \,\mathrm{d}t \tag{27.8}$$

OSI represents a dimensionless number which measures the directional change of WSS during the cardiac cycle. It identifies regions where the WSS vector is reversed from its principal axial direction over each cardiac cycle. Its value changes between 0 and 0.5, with 0 corresponding to uni-directional flow while 0.5 represents purely oscillatory flow.

Note that as indicated in Eq. (27.7), high OSI values are associated with low mean shear stress (e.g. OSI = 0.5 when $\vec{\tau}_{mean} = 0$); this has led to the common use of the '*low and oscillatory shear*' concept in the literature (see Fig. 27.6b, c). It is also worth noting that even though OSI is useful in identifying regions with flow reversal, it is insensitive to the magnitude of shear stress. For instance, sites with low time-averaged shear stress do not necessarily indicate sites of significant OSI; low shear stress levels could be the result of flow expansion without any local flow reversal. Similarly, strongly oscillating flows and slow moving flows, both could exhibit the same OSI [33]. This suggests that while OSI is an important haemodynamic parameter, one should consider studying this index in combination with shear-based metrics to achieve a better understanding of the blood flow in vascular problems.

In the next section, examples of OSI calculated for descending thoracic aorta of a mouse and a rabbit aorta are shown in Fig. 27.8.

27.4.3 Relative Residence Time (RRT)

Relative Residence Time (RRT), initially introduced by Himburg et al. [33], is another common haemodynamic metric which has shown good spatial correlation for the localisation of atherosclerotic disease (see Hoi et al. [34], for example). The motivation behind the use of RRT is based on the importance of the 'residence time' of solutes and formed elements of the blood in the vicinity of vascular endothelium on the atherosclerotic process. At a particular site in a blood vessel, RRT is inversely proportional to a streamwise distance, Δx, that a fully entrained blood particle would travel at a small distance from the wall, y. In the near-wall regions where the viscous effects are significant, once could ignore the spatial variations in shear and therefore,

$$\Delta x = \left| \int_0^T u(y)\, dt \right| = \frac{y}{\mu} \left| \int_0^T \vec{\tau}_w dt \right| \tag{27.9}$$

where $u(y)$ is the streamwise velocity and μ is the blood dynamic viscosity.

Rearranging Eq. (27.7) to solve for $\vec{\tau}_{mean}$ and then substituting into Eq. (27.9) gives:

$$\Delta x = \left(\frac{Ty}{\mu} \right) \times \left[1 - (2 \times \text{OSI}) \right] \times \text{TAWSS} \tag{27.10}$$

For a small distance from the wall, (Ty/c) would be constant, therefore

$$\text{RRT} \sim \frac{1}{\Delta x} \sim \frac{1}{\text{TAWSS} \times \left[1 - (2 \times \text{OSI}) \right]} \tag{27.11}$$

Equation (27.11) shows how RRT is affected by both TAWSS and OSI at any given site. It appears that small OSI values do not have significant effects on RRT, however, when OSI approaches its limit of 0.5, it would have important influence on this metric. Therefore, RRT would be a useful measure of the shear environment for correlative purposes that incorporates the level of the shear and its oscillatory character [33]. Note that since RRT is a relative concept, it is usually normalised using a reference value e.g. RRT at aortic inlet.

Figure 27.8 shows the distribution of the three hemodynamic metrics discussed above, for two different cases.

Acknowledgements The lead author would like to thank all colleagues at the University of Manchester and Manchester Metropolitan University, especially Dr Neil Ashton and Dr Alistair Revell at the University of Manchester who kindly provided some of the figures used in this chapter.

References

1. Steinman DA (2004) Image-based computational fluid dynamics: a new paradigm for monitoring hemodynamics and atherosclerosis. Curr Drug Targets Cardiovasc Haematol Disord 4:183–197
2. Peiffer V, Sherwin SJ, Weinberg PD (2013) Does low and oscillatory wall shear stress correlate spatially with early atherosclerosis? A systematic review. Cardiovasc Res 99:242–250
3. Suo J, Ferrara DE, Sorescu D et al (2007) Hemodynamic shear stresses in mouse aortas: implications for atherogenesis. Arterioscler Thromb Vasc Biol 27:346–351
4. Cebral JR, Mut F, Weir J, Putman C (2011) Quantitative characterization of the hemodynamic environment in ruptured and unruptured brain aneurysms. AJNR Am J Neuroradiol 32:145–151
5. Xiang J, Natarajan SK, Tremmel M et al (2011) Hemodynamic-morphologic discriminants for intracranial aneurysm rupture. Stroke 42:144–152
6. Miura Y, Ishida F, Umeda Y et al (2013) Low wall shear stress is independently associated with the rupture status of middle cerebral artery aneurysms. Stroke 44:519–521. doi:10.1161/STROKEAHA.112.675306
7. Humphrey JD, Taylor CA (2008) Intracranial and abdominal aortic aneurysms: similarities, differences, and need for a new class of computational models. Annu Rev Biomed Eng 10:221–246. doi:10.1146/annurev.bioeng.10.061807.160439.Intracranial
8. Taylor CA, Figueroa CA (2009) Patient-specific modeling of cardiovascular mechanics. Annu Rev Biomed Eng 11:109–134. doi:10.1146/annurev.bioeng.10.061807.160521
9. Andrews KD, Hunt J (2009) Developing smaller-diameter biocompatible vascular grafts. In: Di Silvio L (ed) Cell response to Biomater. Woodhead Publishing, Cambridge, pp 212–236
10. Menu P, Stoltz JF, Kerdjoudj H (2013) Progress in vascular graft substitute. Clin Hemorheol Microcirc 53:117–129
11. Andrews KD, Feugier P, Black RA, Hunt JA (2008) Vascular prostheses: performance related to cell-shear responses. J Surg Res 149:39–46
12. Vara DS, Salacinski HJ, Kannan RY et al (2005) Cardiovascular tissue engineering: state of the art. Pathol Biol 53:599–612
13. Lee B-K (2011) Computational fluid dynamics in cardiovascular disease. Korean Circ J 41:423–430. doi:10.4070/kcj.2011.41.8.423
14. http://rsb.info.nih.gov/ij/
15. https://simtk.org/home/simvascular

16. http://villacamozzi.marionegri.it/luca/vmtk/
17. Cannataro M, Guzzi PH, Tradigo G, Veltri P (2008) A tool for the semiautomatic acquisition of the morphological data of blood vessel networks. IEEE Int Symp Parallel Distrib Proc Appl 2008:837–840. doi:10.1109/ISPA.2008.120
18. Les AS, Shadden SC, Figueroa CA et al (2010) Quantification of hemodynamics in abdominal aortic aneurysms during rest and exercise using magnetic resonance imaging and computational fluid dynamics. Ann Biomed Eng 38:1288–1313. doi:10.1007/s10439-010-9949-x
19. Peric M, Ferziger JH (2002) Computational methods for fluid dynamics, 3rd edn. Springer, Berlin
20. Versteeg HK, Malalasekera W (1995) An introduction to computational fluid dynamics: the finite volume method. Longman Scientific & Technical, Harlow
21. Vincent PE, Plata AM, Hunt AAE et al (2011) Blood flow in the rabbit aortic arch and descending thoracic aorta. J R Soc Interface 8:1708–1719. doi:10.1098/rsif.2011.0116
22. Peiffer V, Sherwin SJ, Weinberg PD (2013) Computation in the rabbit aorta of a new metric – the transverse wall shear stress – to quantify the multidirectional character of disturbed blood flow. J Biomech 46:2651–2658. doi:10.1016/j.jbiomech.2013.08.003
23. Cunningham KS, Gotlieb AI (2005) The role of shear stress in the pathogenesis of atherosclerosis. Lab Invest 85:9–23
24. Fry DL (1969) Certain chemorheologic considerations regarding the blood vascular wall interface with particular reference to coronary artery disease. Circulation 40:38–59
25. Caro CG, Fitz-Gerald JM, Schroter RC (1971) Atheroma and arterial wall shear. Observation, correlation and proposal of a shear dependent mass transfer mechanism for atherogenesis. Proc R Soc Lond B Biol Sci 177:109–159
26. Munson BR, Young DF, Okiishi TH (2005) Fundamental of fluid mechanics. Wiley, New York
27. Koskinas KC, Chatzizisisa YS, Baker AB et al (2009) The role of low endothelial shear stress in the conversion of atherosclerotic lesions from stable to unstable plaque. Curr Opin Cardiol 24:580–590
28. Cecchi E, Giglioli C, Valente S et al (2011) Role of hemodynamic shear stress in cardiovascular disease. Atherosclerosis 214:249–256. doi:10.1016/j.atherosclerosis.2010.09.008
29. Nixon AM, Gunel M, Sumpio BE (2010) The critical role of hemodynamics in the development of cerebral vascular disease. J Neurosurg 112:1240–1253. doi:10.3171/2009.10.JNS09759
30. Janiga G (2013) Computational fluid dynamics challenge for rupture-prediction in intracranial aneurysms. http://www.ovgu.de/isut/LSS/CFD/CFD_Challenge.html
31. Ku DN, Giddens DP, Zarins CK, Glagov S (1985) Pulsatile flow and atherosclerosis in the human carotid bifurcation. Positive correlation between plaque location and low and oscillating shear stress. Arteriosclerosis 5:293–302
32. He X, Ku DN (1996) Pulsatile flow in the human left coronary artery bifurcation: average conditions. J Biomech Eng 118:74–82
33. Himburg HA, Grzybowski DM, Hazel AL et al (2004) Spatial comparison between wall shear stress measures and porcine arterial endothelial permeability. Am J Physiol Heart Circ Physiol 286:H1916–H1922
34. Hoi Y, Zhou Y-Q, Zhang X et al (2011) Correlation between local hemodynamics and lesion distribution in a novel aortic regurgitation murine model of atherosclerosis. Ann Biomed Eng 39:1414–1422